Water Resources Research

RESEARCH ARTICLE
10.1029/2018WR022801

Key Points:
- Plant hydraulics and hydrology are integrated
- Role of alternate water sources in sustaining cottonwoods is assessed
- Susceptibility to different streamflows is predicted

Supporting Information:
- Supporting Information S1
- Data Set S1

Correspondence to:
X. Tai,
xiaonant@buffalo.edu

Citation:
Tai, X., Mackay, D. S., Sperry, J. S., Brooks, P., Anderegg, W. R. L., Flanagan, L. B., Rood, S. B., & Hopkinson, C. (2018). Distributed plant hydraulic and hydrological modeling to understand the susceptibility of riparian woodland trees to drought-induced mortality. *Water Resources Research*, *54*, 4901–4915. https://doi.org/10.1029/2018WR022801

Received 16 FEB 2018
Accepted 23 JUN 2018
Accepted article online 2 JUL 2018
Published online 21 JUL 2018

Distributed Plant Hydraulic and Hydrological Modeling to Understand the Susceptibility of Riparian Woodland Trees to Drought-Induced Mortality

Xiaonan Tai[1], D. Scott Mackay[1], John S. Sperry[2], Paul Brooks[3], William R. L. Anderegg[2], Lawrence B. Flanagan[4], Stewart B. Rood[4], and Christopher Hopkinson[5]

[1]Department of Geography, State University of New York at Buffalo, Buffalo, NY, USA, [2]Department of Biology, University of Utah, Salt Lake City, UT, USA, [3]Department of Geology and Geophysics, University of Utah, Salt Lake City, UT, USA, [4]Department of Biological Sciences, University of Lethbridge, Lethbridge, Alberta, Canada, [5]Department of Geography, University of Lethbridge, Lethbridge, Alberta, Canada

Abstract The mechanistic understanding of drought-induced forest mortality hinges on improved models that incorporate the interactions between plant physiological responses and the spatiotemporal dynamics of water availability. We present a new framework integrating a three-dimensional groundwater model, Parallel Flow, with a physiologically sophisticated plant model, Terrestrial Regional Ecosystem Exchange Simulator. The integrated model, Parallel Flow-Terrestrial Regional Ecosystem Exchange Simulator, was demonstrated to quantify the susceptibility of riparian cottonwoods (*Populus angustifolia, Populus deltoides*, and native hybrids) in southwestern Canada to sustained atmospheric drought and variability in stream flow. The model reasonably captured the dynamics of soil moisture and evapotranspiration in both wet and dry years, including the resilience of cottonwoods despite their high vulnerability to xylem cavitation. Unrealistic predictions of mortality could be generated when ignoring lateral groundwater flow. Our results also illustrated a mechanistic linkage between streamflow and cottonwood health. In the absence of precipitation, normal streamflow could sustain 94% of cottonwoods, and higher streamflows would be required to sustain all of the floodplain cottonwoods. Further, the risk of mortality was mediated by plant hydraulic properties. These results underpin the importance of integrating groundwater processes and plant hydraulics in order to analyze the forest response to sustained severe drought, which could increase in the future due to climate change combined with increasing river water withdrawals.

1. Introduction

Rapidly changing environmental conditions have recently exposed vegetation to extreme drought and caused increased mortality in many ecosystems across the globe (Allen et al., 2015). The impacts of drought on ecosystems can be diverse (Bond et al., 2008), and it is challenging for ecosystem models to predict plant responses to drought (Powell et al., 2013). This can be attributed in part to oversimplified representations of both plant responses to soil drying (Fisher et al., 2017; McDowell et al., 2013) and heterogeneous plant water supply across the landscape (J. S. Clark et al., 2016; Fang et al., 2017).

Current models fail to predict plant response to drought (Hanson et al., 2004; Powell et al., 2013), as they largely rely on simple stress functions with parameters empirically fitted to historic nondrought conditions (Sperry et al., 2016; Xu et al., 2013). Relevant physiological mechanisms are needed for models to reliably predict plant responses to environmental change (McDowell et al., 2013). Plant hydraulics has emerged as a key mechanism for understanding plant water relations (Sack et al., 2016; Venturas et al., 2017), especially under extreme drought (Sperry & Love, 2015). Plant hydraulics provides mechanistically grounded descriptions of water transport along the soil-plant-atmosphere continuum based on measurable plant and soil hydraulic properties (Jackson et al., 2000; Manzoni et al., 2013; Sperry & Love, 2015). Incorporating plant hydraulics has been shown to improve predictions of tree response to drought stress across different species and across the landscape (W. R. Anderegg et al., 2015; Mackay et al., 2015; McDowell et al., 2013; Tai et al., 2017). The success of these studies argues for incorporating plant hydraulics into regional models to gain insights on forest drought responses at the landscape scale (Jackson et al., 2000; Sperry et al., 2016).

Advances in understanding plant response to atmospheric drought highlight the need for improvements in describing belowground processes that mediate water availability (Billings, 2015; Fang et al., 2017; Phillips

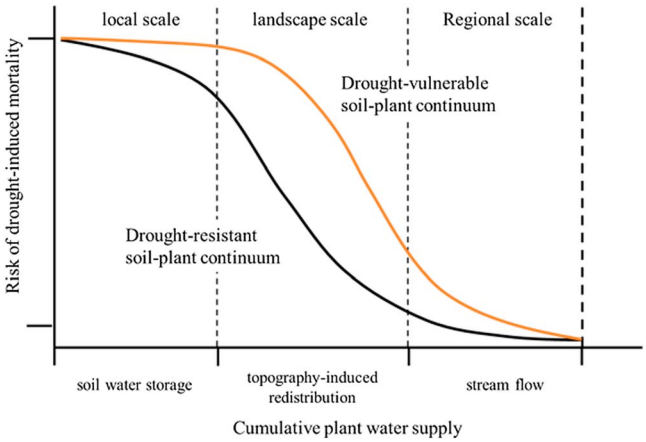

Figure 1. Conceptual diagram showing the contribution of groundwater processes to mediate plant water supply and risk of drought-induced mortality. The *x* axis represents the cumulative plant water sources, with small-scale flow nested inside large-scale flow. The *y* axis represents the ecosystem level mortality risk. Here we simplified groundwater processes into three categories based on the spatial scales of water sources. At local scales, we refer to the vertical flow in the root zone or deeper soil. At landscape scales, we refer to the lateral flow driven by topographic gradients in the absent of long-distance regional flow. At regional scales, we refer to long-distance streamflow driven by large-scale climatologic and geologic factors, as well as stream management along its transportation. Furthermore, plant hydraulic strategies (shown by the differently colored curves) mediate the risk of mortality to a given water supply with drought vulnerable plants requiring a greater water supply to be buffered from drought stress.

et al., 2016). In addition to precipitation infiltration from the top, soils can also be wetted from below or laterally through groundwater processes at local, landscape, and regional scales (Figure 1). At local scales, the water stored in deep soil can sustain plants through multimonth dry seasons after being recharged in the wet season (Miguez-Macho & Fan, 2012; Newman et al., 2006). At landscape scales, groundwater redistributes along topographic gradients to form areas that are consistently wetter than others (Beven & Kirkby, 1979; Dingman, 1994; Fan, 2015; Western et al., 1999). Those wetter areas recently have been shown to support greater productivity and tree growth across a broad range of climates (Swetnam et al., 2017; Thompson et al., 2011). At regional scales, snowmelt from higher elevations supports streamflows and provides remote water sources for the development of riparian vegetation in the semiarid regions (Barnett et al., 2005; Dawson & Ehleringer, 1991).

Groundwater operates across a range of spatial and temporal scales (Schaller & Fan, 2009; Toth, 1963) and can provide sources of plant water that are decoupled and/or asynchronous with the timing of precipitation (Fan, 2015). The consequence of ignoring groundwater hydrology is therefore a failure to account for the different drought intensities experienced by trees within the same or similar climatic conditions, leading to underestimation of the spatial variability of drought impacts and vegetation survival at landscape scales (Fisher et al., 2017). Given its potentially large storage and slow response to climate change (Taylor et al., 2013), groundwater can be critical for mediating the impact of extreme drought on plants and for promoting ecological refugia and seed banks in topographically low areas or along river corridors (Fan, 2015; Krause et al., 2017).

Riparian ecosystems are simultaneously influenced by groundwater processes from local to regional scales (Bergstrom et al., 2016; Cardenas, 2015; Figure 1). Cottonwoods (*Populus* spp.) are a predominant species in riparian ecosystems throughout arid and semiarid regions of North America (Rood et al., 2013). They are expected to be particularly susceptible to the anticipated future droughts given their high vulnerability to xylem cavitation (Tyree et al., 1994) and high sensitivity to declining streamflows (Rood et al., 2013; Scott et al., 1999). Efforts to manage and maintain existing cottonwood forests require quantifying the interaction between their survival and groundwater dynamics (Amlin & Rood, 2003; Flanagan et al., 2017; Scott et al., 1999). Here we present a framework that combines the most recent knowledge of plant hydraulics and variably saturated groundwater modeling to quantify the risk of drought-induced tree mortality across space and time. This integrated model includes much more complete physics-based representations than current approaches and is expected to be more robust when applied to novel environmental conditions (M. P. Clark et al., 2015). By quantifying the mortality risk of a cottonwood ecosystem under different scenarios, we evaluated the following two hypotheses: (1) increasing plant water sources buffers ecosystem vulnerability to drought and (2) ecosystem vulnerability can be further mediated by plant hydraulic traits.

2. Materials and Methods

2.1. Integrated Modeling

An integrated model was developed by coupling a plant physiology model, Terrestrial Regional Ecosystem Exchange Simulator (TREES; Mackay et al., 2015), to a variably saturated groundwater model, PARallel FLOW (ParFlow; Kollet & Maxwell, 2008). TREES has been used to successfully predict tree hydraulic stress and mortality (Johnson et al., 2018; Mackay et al., 2015; McDowell et al., 2013; Tai et al., 2017). It solves plant transpiration and photosynthesis based on meteorological forcing of temperature, precipitation, photosynthetically active radiation, vapor pressure deficit, wind speed, atmospheric CO_2 concentration, and atmospheric pressure. Here TREES was redesigned around a parsimonious model based on plant hydraulics theory

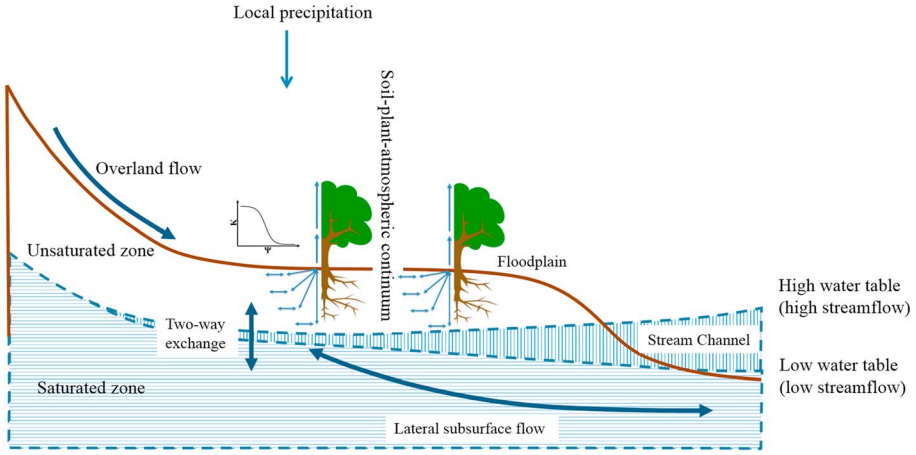

Figure 2. Conceptual diagram of the integrated model coupling a plant physiology model, Terrestrial Regional Ecosystem Exchange Simulator to a variably saturated groundwater model, Parallel Flow. The integrated model, Parallel Flow-Terrestrial Regional Ecosystem Exchange Simulator, captures the three-dimensional water movement in the subsurface and vertically through the soil-plant-atmosphere continuum. It allows the groundwater to laterally redistribute from topographic high to low or from stream channel into the floodplain, driven by the hydraulic gradients.

to predict transpiration (Sperry & Love, 2015; Sperry et al., 2016). This facilitated its integration with a distributed hydrological model, ParFlow, which solves both the surface and subsurface groundwater systems simultaneously. ParFlow is well documented and has also been coupled with the Community Land Model (Kollet & Maxwell, 2008).

In the coupled ParFlow-TREES model, the coupling takes place through soil matric potential and the source/sink terms of evapotranspiration (ET) and infiltration from precipitation. The soil water scheme in the original TREES was replaced with ParFlow, which solves the profile of the soil water potential at each grid cell in the computation domain. TREES derives water uptake from each root layer and feeds this flux back to ParFlow to update the local soil water potential at every time step. The integrated model, ParFlow-TREES, captures the water movement within soils, and along the soil-plant-atmospheric continuum, following water potential gradients both in the lateral directions within the subsurface and vertically within the soil-plant-atmosphere continuum (Figure 2). ParFlow-TREES can be driven by parameters that are spatially uniform or heterogeneous and takes advantage of parallel computation.

Complete details on the equations and parameters in TREES and ParFlow can be found in previous literature (Kollet & Maxwell, 2006, 2008; Mackay et al., 2015; Maxwell & Kollet, 2008; Sperry & Love, 2015; Sperry et al., 2016), and brief summary of the relevant equations is provided here. In the subsurface, ParFlow solves the mixed form of Richards' equation for variably saturated flow (Richards, 1931) in the three spatial dimensions following the notion in (Maxwell et al., 2015)

$$S_s S_w(h)\frac{\partial h}{\partial t} + \varphi S_w(h)\frac{\partial S_w(h)}{\partial t} = \nabla\cdot\boldsymbol{q} + q_r/\lambda, \tag{1a}$$

where the flux term **q** (m/hr) is based on Darcy's law:

$$\boldsymbol{q} = -\boldsymbol{K}_s(x)k_r(h)[\nabla(h+z)\cos\theta_x + \sin\theta_x], \tag{1b}$$

where h is the pressure head (m), z is the elevation (m), x is the index of grid cells in the domain, $\boldsymbol{K}_s(x)$ is the saturated hydraulic conductivity tensor (m/hr), $k_r(h)$ is the relative permeability, Ss is the specific storage (m^{-1}), φ is the porosity, $S_w(h)$ is the relative saturation, q_r is a source/sink term (e.g., precipitation, ET; m/hr) with λ being the thickness of the surface layer (m), and θ is the local slope angle in the lateral directions. The van Genuchten relationships (Van Genuchten, 1980) are used to describe the relative saturation and permeability functions $S_w(h)$ and $k_r(h)$.

Overland flow is represented by the two-dimensional kinematic wave equation (Kollet & Maxwell, 2006):

$$-\boldsymbol{K}_s(x)k_r(h)\cdot\nabla(h+z)=\frac{\partial\|h,0\|}{\partial t}-\nabla\cdot\max\|h,0\|v_{sw}+q_r, \tag{2}$$

where v_{sw} is the two-dimensional, depth-averaged surface-water velocity (m/hr) given by Manning's equation (Chow et al., 1988); max‖h, 0‖ indicates the greater of h and 0. This results in the kinematic wave equation being only active when the pressure at the top cell of the domain is greater than 0 ($h > 0$), and this ponded water is routed following pressure gradients (Kollet & Maxwell, 2006).

The nonlinear, coupled equations of surface and subsurface flow are solved using a parallel Newton-Krylov approach (Jones & Woodward, 2001; Kollet & Maxwell, 2006; Maxwell, 2013). ParFlow solves the variably saturated flow (i.e., saturated and unsaturated groundwater and surface water) in a single matrix based on hydrodynamic principles, without a priori specification of the types of flow in certain portion of the domain. While this yields a challenging computational problem, ParFlow takes advantage of a multigrid preconditioner (Ashby & Falgout, 1996) and parallel computation (Kollet et al., 2010).

The source/sink term q_r is expressed as

$$q_r = I - E - T, \tag{3}$$

where I is the flux of water infiltrating at the land surface (m/hr), E is soil evaporation (m/hr), and T is transpiration (m/hr). E is calculated using the Penmann-Monteith equation, with the conductance term assumed to be proportional to soil water content using an analog for Darcy's law (Millar et al., 2017). T is solved by the parsimonious plant hydraulics scheme in TREES, which predicts a steady-state relation between T and xylem pressure (P_c) at a given soil water potential (P_s; equation (4); Sperry et al., 2016). The decline of hydraulic conductance (k) from its maximum (k_{max}) to more negative P is described using a two-parameter Weibull function, known as vulnerability curves (equation (5)), for xylem components (leaf, stem, and root) and a van Genuchten function (Van Genuchten, 1980) for the rhizosphere, which refers to the soil around each root through which water moves down a pressure gradient from the bulk soil.

$$T = \int_{P_{up}}^{P_{down}} k(P)\mathrm{d}P, \tag{4}$$

$$k(P) = k_{max}e^{\left[-(P/b)^c\right]}. \tag{5}$$

Following the hydraulic model of Sperry and Love (Sperry & Love, 2015; Sperry et al., 2016), stomata are assumed to regulate the pressure drop $\Delta P = P_s - P_c$ based on the fractional drop in whole plant-soil hydraulic conductance from its maximum (k/k_{max}):

$$\Delta P = \Delta P' k/k_{max}, \tag{6}$$

where $\Delta P'$ is the unregulated pressure drop, given by the multiplication of vapor pressure deficit, D, and the maximum diffusive conductance parameter, G_{max}. This regulated ΔP yields the regulated values for T. G_{max} is alternatively coupled to the photosynthesis routine of TREES to capture the response of diffusive conductance to other factors such as light and temperature, given by

$$G'_{max} = a\frac{A}{c_a - c_i}, \tag{7}$$

where A is photosynthetic carbon assimilated per unit leaf area based on a photosynthesis model (Farquhar et al., 1980); a = 1/1.6 is a molar conversion constant between water vapor and CO_2 conductance; c_a and c_i are molar fractions of CO_2 in the leaf surface and in the leaf intercellular air spaces, respectively. The minimum of G_{max} and G'_{max} is used at every time step. This plant hydraulics routine was implemented as a module in TREES, with the meteorological forcing and other parameters similar to the original TREES model (Mackay et al., 2015). Major model parameters and values used in this study are listed in Table 1.

2.2. Data and Model Setup

We examined the water status of a natural riparian cottonwood forest (*Populus angustifolia, Populus deltoides*, and native hybrids) along a 3-km river corridor within the Oldman River valley near Lethbridge, Alberta,

Table 1
Major Inputs of the Model and Values Used in This Study

Model parameter	Baseline values (test values)[a]	Sources
(a) TREES parameters		
Weibull vulnerability curve parameter [b, c]	[2.03, 5.25] ([0.95, 1.02][b])	Measured for xylem and assumed to be the same for roots and leaves; test values were extracted from Tyree et al. (1994)
Maximum whole plant hydraulic conductance per leaf area (K_{max})	6.5 mmol·s^{-1}·m^{-2}·MPa (22 mmol·s^{-1}·m^{-2}·MPa)[b]	Estimated
Maximum diffusive conductance to water vapor (G_{max})	0.2 mol·s^{-1}·m^{-2} (0.4 mol·s^{-1}·m^{-2}·MPa)[b]	Estimated
Rooting depth	1 m (2 m)[c]	Rood et al. (2011); test value was assumed
(b) ParFlow parameters		
Domain	50 × 18 × 20	
Grid size	60 × 60 × 0.5 m	
Van Genuchten parameters [a, n]	[7.5, 1.89] for top 2 m and [14.5, 2.68] for bottom 8 m	Leij et al. (1996)
Saturated permeability	0.0442 m/hr for top 2 m and 9 m/hr for bottom 8 m	Fleckenstein et al. (2006)
Saturated soil moisture	0.53	Observed
Residual soil moisture	0.1	Observed
Manning's coefficient	2 × 10^{-6} hr/m$^{1/3}$	Assumed
(c) Initial and boundary condition		
Boundary condition	No flow except for the surface allowing overland flow when the water table rises to the land surface	
Initial condition	Spin-up for one growing season using the meteorological forcing and streamflow observed for the wet year 2014 without simulating trees	

Note. ParFlow = Parallel Flow; TREES = Terrestrial Regional Ecosystem Exchange Simulator.
[a]Baseline values were used to compare against observations at the study site; test values were used to evaluate its influence over model output. [b]For the xylem vulnerability test; the higher xylem vulnerability was prescribed along with higher K_{max} and G_{max} values. [c]For the deeper rooting depth test.

Canada (49.702°N, 112.863°W). This is a semiarid prairie region with streamflows originating in the Rocky Mountain (Rood et al., 2013). Observations of meteorological variables such as photosynthetically active radiation, precipitation, temperature, wind speed, vapor pressure deficit, streamflow, and leaf area index, ET, and total water in the top 2.50-m depth of soil were made during both wet (2014) and dry (2015) years with contrasting May–September cumulative precipitation (2014: 362 mm; 2015: 181 mm) and average streamflow rates (2014: 265 m^3/s; 2015: 61 m^3/s; Flanagan et al., 2017).

ParFlow-TREES was initiated with parameter values listed in Table 1 and the model domain shown in Figure 3. Branch xylem vulnerability to cavitation was measured and was assumed to be the same for leaf, stem, and root segments. K_{max} and G_{max} were estimated from observed ET. Rooting depth near the study site was reported to be around 1.0 m (Rood et al., 2011). ParFlow-TREES has the capacity of prescribing spatially heterogeneous parameters and those parameters were assigned to the extent that information was available. Land cover types were assigned based on a digital height model generated from airborne lidar data (Hopkinson et al., 2005) that differentiated among trees, soil, and stream. Tree-covered grid cells were simulated with plant hydraulics and soil evaporation, soil cells were simulated with only soil evaporation, and stream cells were simulated without ET. The average of ET and soil moisture from cells roughly falling within the footprint of the eddy covariance flux tower was used to compare against observations (Flanagan et al., 2017). To simplify computation, a smoothed topography was imposed to distinguish cells representing the stream channel, riverbanks, and floodplains (Figure 2b). All cells had a slope of 0.01 m/km in the direction of the river flow. We focused on modeling the stream-floodplain interaction and assumed a negligible contribution from upslope drainage, as this ecosystem was mostly influenced by alluvial groundwater (Rood et al., 2013; Willms et al., 1998). A temporally varying streamflow rate was prescribed at the upstream end (Figure 3a) based on the closest gauge station (water ID station 05AD007, data archived by the Water

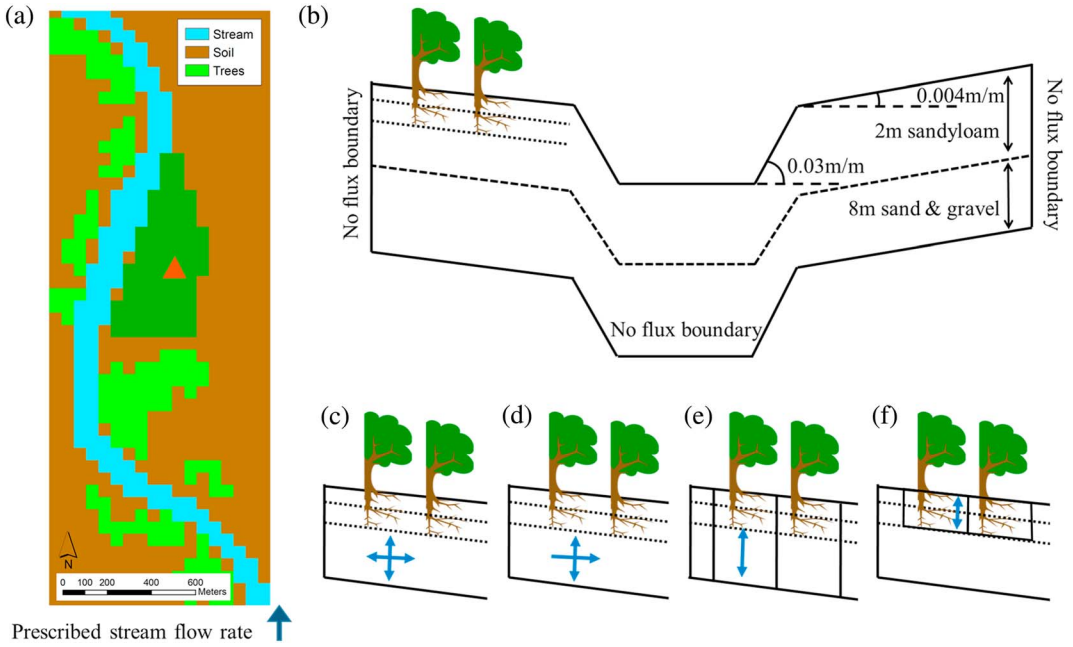

Figure 3. Model setup in the planar (a) and profile (b) directions. The model domain was discretized into 50 × 18 × 20 cells with a uniform cell dimension of 60 × 60 × 0.5 m, covering a river corridor area of 3 by 1.08 km. In (a), colors represented the land cover types of the model, including trees, soils, and stream channels. Dark green cells represented trees falling within the footprint of the eddy covariance flux tower (red triangle). Streamflow rates were prescribed at the upstream end designated by the dark blue arrow. In (b), the vertical domain was discretized to 20 layers for a total depth of 10 m. The top 2 m represented a finer textured substrate of sandy loam, and the bottom 8 m represented a coarse substrate of sand and gravel. Riverbanks have a profile slope of 0.03 m/m, and floodplains have a profile slope of 0.004 m/m. All cells had a slope of 0.01 m/km in the river flow direction. Four characterizations of plant water sources (c–f) were compared using model simulations. (c) The 3D_GW_Stream simulation where three-dimensional water flow was solved. (d) The 3D_GW simulation where streamflow was eliminated from the simulation, while soil parameters were the same as 3D_GW. (e) The Vert_GW simulation where groundwater flows only in the vertical direction by setting lateral soil permeability to zero. (f) The RootZone simulation where trees rely solely on root zone storage by further setting soil permeability beyond the root zone to zero. Blue arrows within (c)–(f) represent the water flows.

Survey of Environment Canada), situated at the downstream edge of the study domain. Measured growing season meteorological forcing from 1 May to 3 September for a total of 125 days in both years was applied uniformly across the domain.

2.3. Numerical Experiments

ParFlow-TREES provided a framework where mechanisms were isolated and evaluated experimentally by manipulating model inputs. Here we focused on two hypotheses (Table 2). First, we assessed if increasing plant water sources could buffer drought stress for the ecosystem by adjusting soil permeability parameterization and incoming streamflow (Table 2 and Figures 3c–3f). RootZone, Vert_GW, 3D_GW, and 3D_GW_Stream represented progressively increasing water sources that plants can access. Using these configurations, we imposed an extreme drought that eliminated precipitation from the 2015 meteorological conditions and repeated for 10 growing seasons (May–September). The observed 2015 streamflow (average rate: 55 m^3/s) was multiplied by different factors to create a wide range of flow regimes (Table 2). We focused on growing seasons based on the strong association between groundwater and cottonwood growth during the growing season (Rood et al., 2013; Shepherd et al., 2010). Although this ignored the potential replenishment of groundwater storage during winter and early spring, it represented an extreme scenario with carry-over effects of sustained drought between years. To characterize the risk of drought-induced mortality, we reported the average percentage loss of whole-plant hydraulic conductance (PLK) during the growing season for every year. We also reported the percentage of modeled tree cells across the landscape experiencing a PLK greater than 60% for each year, based on previous studies suggesting that 60% is a starting point, beyond which the probability of mortality increased dramatically (Adams et al., 2017; McDowell et al., 2013).

Table 2
Description of Hypotheses and Corresponding Setup of the Numerical Experiments

Hypothesis	Groundwater setup	Plant parameters	Streamflow multiplying factor
Increasing plant water sources buffers drought stress	3D_GW_Stream	Baseline	0.1, 0.5, 1, 2
	3D_GW	Baseline	0
	Vert_GW	Baseline	0
	RootZone	Baseline	0
Plant hydraulic traits mediate sensitivity to water sources and water supply	RootZone, Vert_GW, 3D_GW, 3D_GW_Stream	Vulnerable xylem Deep roots	0.0, 0.1, 0.5, 1, 2

Note. 3D_GW_Stream denoted the model setup solving the full three-dimensional water flow; 3D_GW represented lateral groundwater flow driven by topography only; Vert_GW denoted the model setup that only allowed vertical flow; RootZone denoted the model setup that solved the flow in the vertical direction and within the root zone.

To evaluate the second hypothesis, we repeated the first experiment, but with different sets of plant hydraulic traits including more vulnerable xylem and deeper rooting depth (Table 2). We expect that a more vulnerable xylem would make the system more sensitive to drought and changes in water sources and a deeper rooting depth would make the system less sensitive. The impact of other factors, such as topography, substrate texture and permeability, and vegetation distribution, has been previously reported (Atchley & Maxwell, 2011; Rihani et al., 2010). Although not exhaustive, these numerical experiments provide some insights about the system and address the following questions: (1) How do different groundwater processes buffer plant water stress during drought? (2) What magnitudes of streamflow sustain current cottonwood forests during drought? (3) How do different water sources and plant hydraulic traits interact to influence forest sensitivity to drought-induced mortality?

3. Results

3.1. Model Evaluation in the Wet and Dry Years

Parflow-TREES with the 3D_GW_Stream scenario reasonably captured the dynamics of ET and soil water both in the wet (2014) and dry (2015) years (Figure 4). In 2014, soil water was recharged by high streamflow in the early growing season, whereas in 2015 soil water declined monotonically. In spite of the much lower precipitation in year 2015, the total ET was roughly comparable in both years.

3.2. Sensitivity to Multiyear Extreme Drought

As drought progressed over time, PLK increased and the seasonal total ET decreased (Figure 5). But different sensitivities were predicted when considering alternative plant water sources. When solely relying on water stored in the root zone (Figure 5, RootZone, red lines), trees experienced a mean PLK of 50% in the first year and over 90% in subsequent years. Groundwater subsidy provided a buffer against drought stress, but

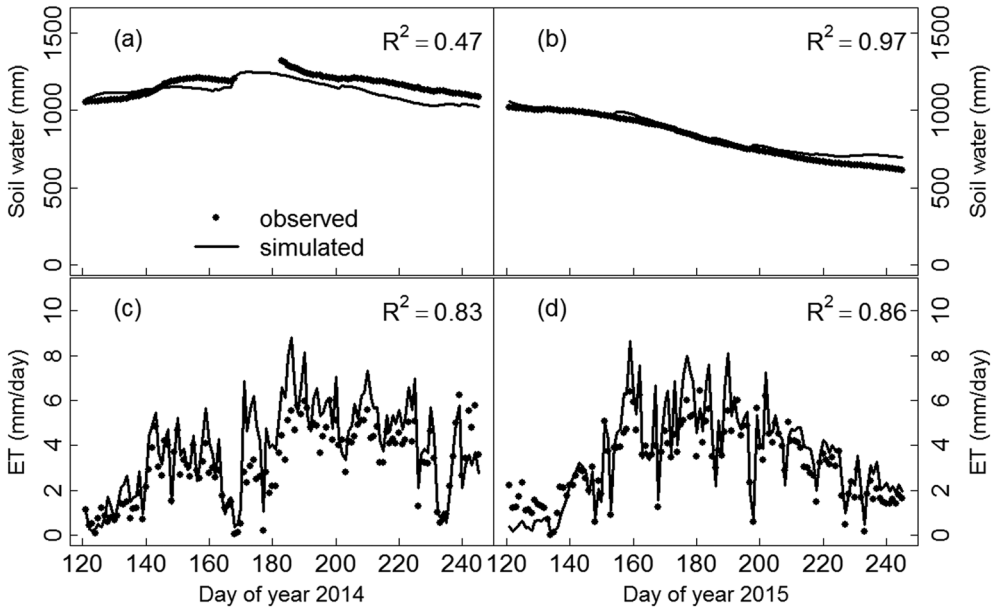

Figure 4. Simulated (solid lines) and observed (solid dots) daily soil water (a, b) and ET (c, d) versus date of year in 2014 (a, c) and 2015 (b, d). Soil water is presented as the total water within the top 2.5 m of soil. R^2 of observations versus the mean of predictions from model cells falling within the footprint of the eddy covariance measurements is presented.
ET = evapotranspiration.

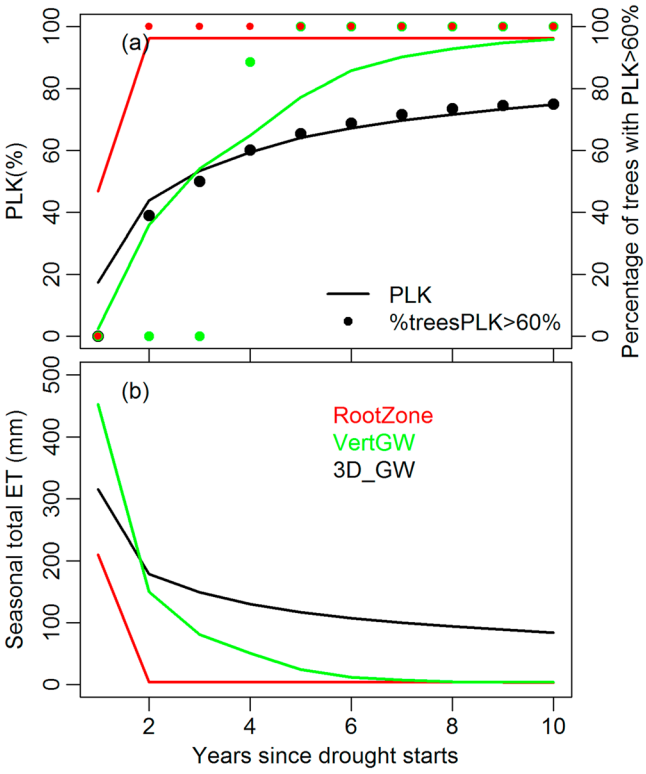

Figure 5. Predictions of seasonal average PLK (a) and total ET (b) during the 10 years of drying down without precipitation and incoming streamflow. Colors represented the three alternate representations of plant water sources by manipulating the model parameter, saturated permeability. RootZone represented plants taking water solely from root zone storage; Vert_GW represented plants taking water from both root zone and beyond root zone through vertical flow, but lateral flow was ignored; 3D_GW represented plants taking water from the integrated 3-D water flow. The mean values across the landscape were presented. Solid dots represented the fraction of trees experiencing a PLK over 60% across the landscape for a given year. Different dot sizes were used for easier visualization. ET = evapotranspiration; PLK = percentage loss of hydraulic conductance.

differences could be observed between the predictions of Vert_GW and 3D_GW (Figure 5, green versus black lines). The Vert_GW setup that only considered the vertical flow predicted lower PLK in the first 3 years and higher PLK in subsequent years.

Assuming that tree mortality occurred when the associated PLK exceeded 60%, the RootZone setup predicted that all trees would likely have died by the second year of drought. The Vert_GW setup predicted no mortality within the first 3 years of drought and 100% mortality after the fourth year (Figure 5a, red and green dots). By contrast, the 3D_GW predicted mortality to progress gradually over time (Figure 5a, black dots), starting with trees located furthest from the stream channel (Figure 6).

Without streamflow, groundwater flow was mostly governed by topographic gradients from high to low elevation. Trees located at higher topographic positions lost water to trees at lower positions, experienced a deeper water table, and had higher PLK even during the first 3 years of drought (Figure 7). As drought sustained, more trees became stressed with increasing PLK. But a small fraction of trees at lower elevation near the stream channel remained buffered from drought stress. Without lateral water redistribution, the Vert_GW model setup predicted little spatial variations in PLK and all trees were dead by the fifth year of drought (Figure 5).

3.3. Drought Stress Mediated by Streamflow

In the absence of precipitation, higher streamflow raised the water table and reduced the mean values of PLK (Figure 8), as groundwater predominately flowed from stream into the floodplain following the hydraulic gradients. But some trees located away from the stream still experienced a PLK greater than 60% (Figures 8 and 9). The simulations suggested that 6% cottonwoods could be threatened if the streamflow was to be maintained at the dry year level (multiplier = 1). If the streamflow was doubled (multiplier = 2), then all trees were buffered from water stress even if there was no precipitation.

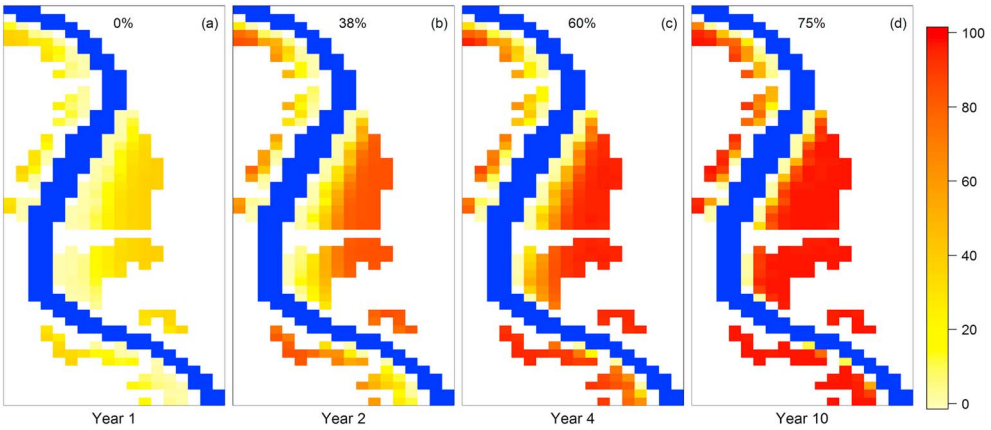

Figure 6. Spatial distribution of seasonal average PLK predicted by the 3D_GW setup, as drought progressed into the (a) first, (b) second, (c) fourth, and (d) tenth years of the extreme drought experiment with no precipitation and no streamflow. Color gradients represent the magnitude of PLK. Blue cells represented the stream channel. The fractions of tree cells experiencing a PLK over 60% for a given year were presented as numbers in the top of each snapshot. PLK = percentage loss of hydraulic conductance.

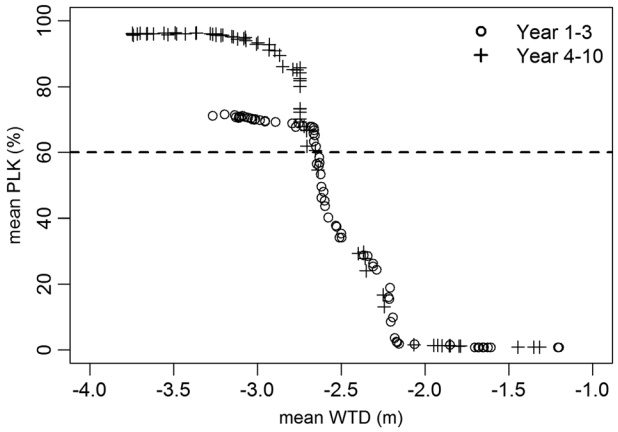

Figure 7. Temporal means of WTD versus seasonal PLK for individual trees simulated in the extreme drought experiment during the first 3 years of drought (open circles) and during the latter 7 years of drought (crosses). Every dot represented a single tree cell, and only cells falling within the footprint of the eddy covariance measurements are shown for easier visualization.
PLK = percentage loss of hydraulic conductance; WTD = water table depth.

3.4. Integrated Effects of Relevant Processes in Predicting Sensitivity to Drought

The two-way lateral redistribution of groundwater from topographic high to low and from the stream into the floodplain zone was shown to buffer cottonwood against sustained severe drought (Figure 10, orange lines). This mediating influence was negligible if the drought was limited to a single growing season when the alluvial aquifer storage was still high (Figure 10, light blue line). As expected, plant hydraulic traits mediated the sensitivity to water sources (Figure 10, different symbols). Given the same water supply, cottonwoods with vulnerable xylem were at greater risk of mortality, and growing deeper roots reduced the risk of mortality.

4. Discussion

4.1. Model Evaluation in the Wet and Dry Years

The much lower precipitation in the dry year 2015 had little impact on ET (Figure 4), indicating that plants were taking water from sources other than precipitation. This has been attributed to the large storage capacity of the floodplain substrate (Flanagan et al., 2017) and the relatively shallow water table sustained by streamflow (Rood et al., 2013; Scott et al., 1999). Storage could effectively buffer cottonwoods against isolated dry years, although reduced growth has been reported when the drought was severe (Schook et al., 2016).

4.2. Sensitivity to Multiyear Extreme Drought

In spite of the extremely dry conditions and the highly vulnerable xylem of cottonwood (Tyree et al., 1994), 3D_GW predicted a gradual increase of mortality risk over time (Figures 5 and 6). The predicted pattern fell within the realm of previously documented cottonwood declines at other sites suggesting that mature cottonwoods were resilient (Andersen, 2016; Braatne et al., 2007), and that cottonwood decline was gradual, spanning several years to decades (Rood et al., 2003, 1995). Trees located lower in elevation received subsidy at the expense of sacrificing trees at higher positions (Figure 7), similar to the study at a headwater catchment (Shen et al., 2013). The fraction of trees receiving subsidy became smaller over time (Figure 6), resulting in a pattern of narrowing forest bands on the floodplain that has been reported (Cordes et al., 1997; Rood et al., 2003). High PLK was predicted when the water table fell beyond a depth of 3 m (Figure 7). This agreed with the previous findings that cottonwoods were generally restricted to streamside bands where depth to the water table was no greater than 3.5 m (Busch et al., 1992; Horton et al., 2001; Scott et al., 1999), although cottonwoods can survive at places where the water table is much deeper (Zimmermann, 1969).

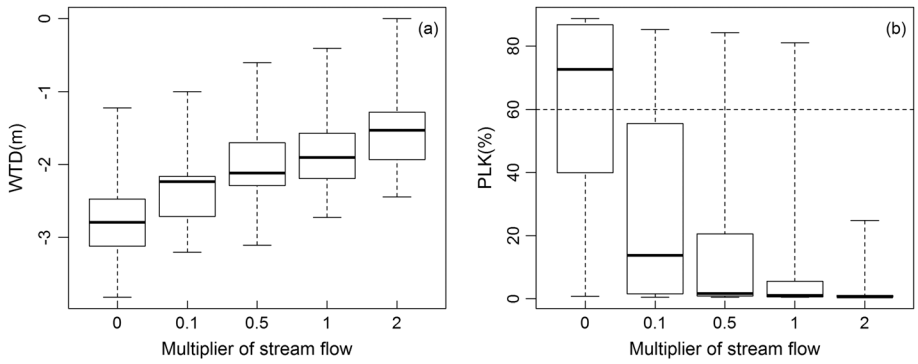

Figure 8. WTD (a) and seasonal average PLK (b) during the 10th growing season with no precipitation and varying magnitudes of streamflow. The observed streamflow during the dry year (2015) was adjusted by multiplying factors of 0, 0.1, 0.5, 1, and 2, respectively. These streamflow scenarios corresponded to a mean discharge rate of 0.0, 6.1, 30.5, 61, and 122 m^3/s, respectively. The box and whisker plots showed the median, upper, and lower quartiles of the data, with the whiskers extending to the most extreme data point. PLK = percentage loss of hydraulic conductance; WTD = water table depth.

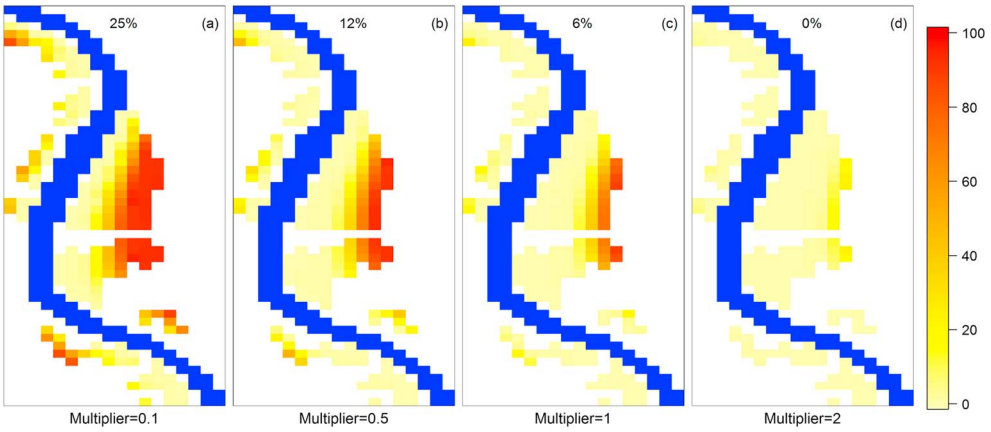

Figure 9. Spatial distribution of seasonal average PLK during the 10th growing season with different magnitudes of streamflow that were adjusted by a multiplying factor of (a) 0.1, (b) 0.5, (c) 1, and (d) 2 based on the observed streamflow during 2015. These scenarios corresponded to a mean discharge rate of 6.1, 30.5, 61, and 122 m^3/s, respectively. Color gradients represent the magnitude of PLK. Blue cells represented the stream channel. The fraction of tree cells experiencing a PLK over 60% for a given year was also presented as numbers in the top of every snapshot. PLK = percentage loss of hydraulic conductance.

RootZone and Vert_GW predicted a step change from zero to total mortality across the landscape (Figure 5), which is probably unrealistic (Fisher et al., 2017). In particular, the Vert_GW configuration mimics the effects of a routine that has been widely adopted in current land surface models (M. P. Clark et al., 2015; Fan, 2015). But our results demonstrated that it might underpredict the mortality risk of trees at higher positions early in the drought and overpredict the mortality risk of trees at lower positions late in the drought. Consequently, this representation of plant water supply could be insufficient for predicting tree survival/mortality at landscape scales.

4.3. Drought Stress Mediated by Streamflow

Incorporating streamflow (Figures 8 and 9) demonstrated the hydrologic linkage between riparian cottonwoods and stream discharge in semiarid regions where local precipitation is insufficient to support trees (Rood et al., 2013). The spatial average PLK dropped from 73% to less than 20% when streamflow increased

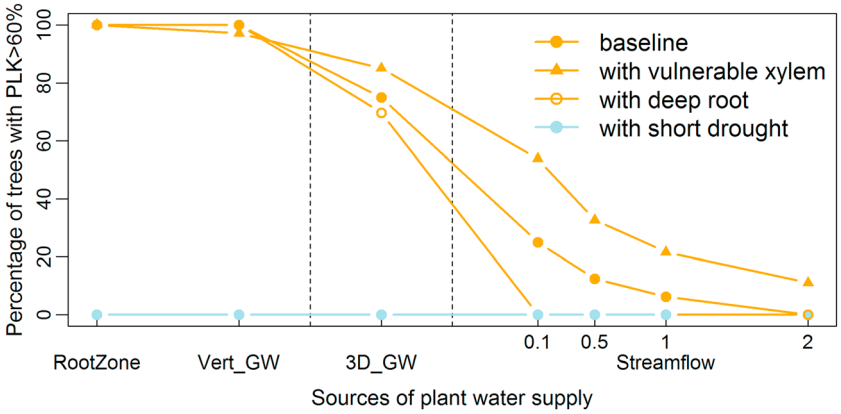

Figure 10. Percentage of tree grid cells experiencing PLK over 60% predicted by different representations of plant water sources from RootZone, Vert_GW, 3D_GW, and stream-floodplain interaction associated with various magnitudes of streamflow (Streamflow, numbers represent the multipliers used to rescale the observed streamflow in 2015), for the tenth year (orange lines) and first year (light blue line) since drought started. Dot symbols represented different plant hydraulic traits being tested. Filled circles represented the baseline model parameter, filled triangles represented cottonwoods with more vulnerable xylem, and open circles represented cottonwoods with deeper rooting depth. PLK = percentage loss of hydraulic conductance; RootZone = root zone storage; Vert_GW = vertical water flow; 3D_GW = lateral redistribution induced by topography.

from 0% to 10% of the magnitude in year 2015 (Figure 9b). This is likely to be related to the high transmissivity of riparian substrates characterized by gravels so that water can quickly move into the floodplain (Amlin & Rood, 2003). Notably, higher streamflow was required to replenish places that were distant from the stream (Friedman & Lee, 2002; Leblanc et al., 2012) and to sustain trees growing in these positions with elevation ~1 m higher than the riverside trees (Figures 8b and 9d).

Future drought in the headwater catchments could result in thin snowpack and have a profound influence on the health of downstream riparian forests (Braatne et al., 2007; Rood et al., 1995), especially if it coincides with a reduction in local precipitation. The impact of drought would be enhanced by increased demands for river water diversion (Dijk et al., 2013). In turn, riparian ecosystems could be more vulnerable if there was not sufficient streamflow to compensate for reduced precipitation and to recharge the local alluvial groundwater.

4.4. Integrated Effects of Relevant Processes in Predicting Sensitivity to Drought

The dependency of tree health on groundwater sources diminished when the drought was short and the storage was high (Figure 10, light blue line). Similarly, the reliance of cottonwoods on streamflow could also be dampened when there is sufficient water supply from local precipitation (Busch et al., 1992; Scott et al., 1999; Snyder & Williams, 2000). Our results have implications for different conceptualizations of plant water sources: They can give similar predictions under wet conditions but dramatically different answers during sustained extreme drought. Given the anticipated future with more extreme, longer-term or frequent drought and prolonged low streamflow conditions (Mishra et al., 2010; Sheffield & Wood, 2008), integrating all relevant processes therefore has the potential of being more robust compared to the simpler representations in current models for quantifying the risk of drought-induced forest mortality.

Consistent with studies showing different tolerances to low water potentials across cottonwood genotypes (Kranjcec et al., 1998; Tyree et al., 1994), ParFlow-TREES predicted higher PLK for trees with a more vulnerable xylem under the same hydro-climatic conditions (Figure 10). Trees with deeper roots had greater access to soil water storage (Johnson et al., 2018) and lower reliance on high streamflow (Figure 10). These results reinforce the growing evidence from both field and modeling studies that accurate evaluation of forest vulnerability to future drought hinges on the integration of plant hydraulic properties with hydrological processes (Jackson et al., 2000; Tai et al., 2017).

4.5. Methodological Limitations

Our numerical experiments evaluating the mortality risk of a riparian cottonwood forest serve as a useful illustration of groundwater controls over plant responses to drought. As with any modeling effort, results come with a number of limitations.

First, we focused on the magnitude of streamflow and mature cottonwood trees. Extreme flooding events and variations in streamflow seasonality have been recognized as important processes for cottonwood recruitment and seedling establishment (Braatne et al., 2007; Harner & Stanford, 2003; Lytle & Merritt, 2004; Rood et al., 2008; Scott et al., 1997). Furthermore, we used a threshold of 60% seasonal average PLK to report the risk of cottonwood mortality based on the previous studies (Adams et al., 2017; McDowell et al., 2013). But a different value might be needed depending on the various symptoms of *decline* (e.g., branch sacrifice, reduced sexual and vegetative reproduction, and slower growth; Rood et al., 2000; Scott et al., 1999), as well as plant traits such as the ability to recover from embolism (Adams et al., 2017; McDowell et al., 2013). Those aspects, although beyond the scope of the current study, should be incorporated to improve predicting the flow requirement for cottonwood restoration.

Second, the model domain was confined to the river and riparian floodplain. Although the study site was primarily influenced by alluvial groundwater (Rood et al., 2013; Willms et al., 1998), upslope drainage might contribute significant amount of water for plants developing along some rivers (Winter, 1998). Similarly, different cross-section geometries of the model domain might cause a different distribution pattern of water supply.

Third, we assumed no flux boundary conditions that only allowed water to leave the domain as overland flow through the stream channel (Schaller & Fan, 2009) and eliminated potential water exchanges with the deeper, regional-scale groundwater. Although the same boundary condition was applied to all model simulations and should not affect the relative importance of alternate water sources in mediating drought

impact, it resulted in the model prediction of cottonwood survival after 10 years of no precipitation and no streamflow (Figure 6d), which was less likely to happen in the real world.

Lastly, although ParFlow-TREES has the capacity to use spatially variable input of hydrologic and plant physiological parameters, they were assumed to be uniform in this study due to the lack of spatial information. But heterogeneity in hydraulic conductivity and geomorphic structures in particular has been shown to be important for characterizing the river-aquifer (i.e., hyporheic) exchange (Cardenas, 2015; Frei et al., 2009). Furthermore, plants are likely to adapt to local habitat by altering their physiological or morphological traits (L. D. Anderegg & HilleRisLambers, 2015; Bréda et al., 2006; Hacke et al., 2000) over time and/or across space. Improved characterization of the variability in subsurface properties, traits of different individual trees, and different tissues within the same tree will be important to accurately quantify ecosystem sensitivity to future hydroclimatic conditions. Ongoing efforts at Critical Zone Observatories and global plant trait databases might appear to offer promising means for getting such information for subsurface (Billings, 2015; Fan, 2015) and plant trait plasticity (Fan et al., 2017; Kattge et al., 2011).

5. Conclusions

We presented ParFlow-TREES, an integrated model that combined recent developments in plant hydraulics and groundwater hydrology, to mechanistically quantify the heterogeneous forest response to drought at the landscape scale. Model experiments with a cottonwood riparian forest demonstrated the interplay between groundwater processes and plant hydraulics in mediating the risk of mortality under sustained drought conditions. ParFlow-TREES also illustrated a mechanistic link between regional-scale streamflow and the ecological consequences of tree survival at the landscape scale. Quantifying their interaction will be informative for management practices targeting the resilience and/or restoration of riparian ecosystems.

Acknowledgments
We thank Ying Fan from Rutgers University and two anonymous reviewers for their comments that greatly helped improve the manuscript. We also thank Reed Maxwell from Colorado School of Mines for informative discussions. This work was funded by the National Science Foundation (NSF) through grants IOS 1450679 and IOS 1450650. This research was also part of the Functional Flows: A Practical Strategy for Healthy Rivers project and was supported by grants from Alberta Innovates-Energy and Environment Solutions, the Natural Sciences and Engineering Council of Canada - Discovery Grant Program, and Conoco Phillips Canada. David Ellis (City of Lethbridge) and Coreen Putman (Helen Schuler Nature Centre, Lethbridge) provided permission to conduct research in the Nature Centre grounds. The statements made in this manuscript reflect the views of the authors and do not necessarily reflect the views of the funding agencies. Data used in this study are available as Data Set S1.

References

Adams, H. D., Zeppel, M. J., Anderegg, W. R., Hartmann, H., Landhäusser, S. M., Tissue, D. T., et al. (2017). A multi-species synthesis of physiological mechanisms in drought-induced tree mortality. *Nature Ecology & Evolution*, *1*(9), 1285–1291. https://doi.org/10.1038/s41559-017-0248-x

Allen, C. D., Breshears, D. D., & McDowell, N. G. (2015). On underestimation of global vulnerability to tree mortality and forest die-off from hotter drought in the Anthropocene. *Ecosphere*, *6*(8), 1–55.

Amlin, N. M., & Rood, S. B. (2003). Drought stress and recovery of riparian cottonwoods due to water table alteration along Willow Creek, Alberta. *Trees*, *17*(4), 351–358.

Anderegg, L. D., & HilleRisLambers, J. (2015). Drought stress limits the geographic ranges of two tree species via different physiological mechanisms. *Global Change Biology*.

Anderegg, W. R., Flint, A., Huang, C.-y., Flint, L., Berry, J. A., Davis, F. W., et al. (2015). Tree mortality predicted from drought-induced vascular damage. *Nature Geoscience*, *8*(5), 367–371. https://doi.org/10.1038/ngeo2400

Andersen, D. C. (2016). Flow regime effects on mature Populus fremontii (Fremont cottonwood) productivity on two contrasting dryland river floodplains. *The Southwestern Naturalist*, *61*(1), 8–17. https://doi.org/10.1894/0038-4909-61.1.8

Ashby, S. F., & Falgout, R. D. (1996). A parallel multigrid preconditioned conjugate gradient algorithm for groundwater flow simulations. *Nuclear Science and Engineering*, *124*(1), 145–159. https://doi.org/10.13182/NSE96-A24230

Atchley, A. L., & Maxwell, R. M. (2011). Influences of subsurface heterogeneity and vegetation cover on soil moisture, surface temperature and evapotranspiration at hillslope scales. *Hydrogeology Journal*, *19*(2), 289–305. https://doi.org/10.1007/s10040-010-0690-1

Barnett, T. P., Adam, J. C., & Lettenmaier, D. P. (2005). Potential impacts of a warming climate on water availability in snow-dominated regions. *Nature*, *438*(7066), 303–309. https://doi.org/10.1038/nature04141

Bergstrom, A., Jencso, K., & McGlynn, B. (2016). Spatiotemporal processes that contribute to hydrologic exchange between hillslopes, valley bottoms, and streams. *Water Resources Research*, *52*, 4628–4645. https://doi.org/10.1002/2015WR017972

Beven, K., & Kirkby, M. (1979). A physically based, variable contributing area model of basin hydrology/un modèle à base physique de zone d'appel variable de l'hydrologie du bassin versant. *Hydrological Sciences Journal*, *24*(1), 43–69. https://doi.org/10.1080/02626667909491834

Billings, S. A. (2015). 'One physical system': Tansley's ecosystem as Earth's critical zone. *New Phytologist*, *206*(3), 900–912.

Bond, N. R., Lake, P., & Arthington, A. H. (2008). The impacts of drought on freshwater ecosystems: An Australian perspective. *Hydrobiologia*, *600*(1), 3–16. https://doi.org/10.1007/s10750-008-9326-z

Braatne, J. H., Jamieson, R., Gill, K. M., & Rood, S. B. (2007). Instream flows and the decline of riparian cottonwoods along the Yakima River, Washington, USA. *River Research and Applications*, *23*(3), 247–267. https://doi.org/10.1002/rra.978

Bréda, N., Huc, R., Granier, A., & Dreyer, E. (2006). Temperate forest trees and stands under severe drought: A review of ecophysiological responses, adaptation processes and long-term consequences. *Annals of Forest Science*, *63*(6), 625–644. https://doi.org/10.1051/forest:2006042

Busch, D. E., Ingraham, N. L., & Smith, S. D. (1992). Water uptake in woody riparian phreatophytes of the southwestern United States: A stable isotope study. *Ecological Applications*, *2*(4), 450–459. https://doi.org/10.2307/1941880

Cardenas, M. B. (2015). Hyporheic zone hydrologic science: A historical account of its emergence and a prospectus. *Water Resources Research*, *51*, 3601–3616. https://doi.org/10.1002/2015WR017028

Chow, V. T., Maidment, D. R., & Mays, L. W. (1988). Applied hydrology. In R. Eliassen, P. H. King, & R. K. Linsley (Eds.), *McGraw-Hill series in water resources and environmental engineering* (572 pp.). McGraw-Hill, Inc.

Clark, J. S., Iverson, L., Woodall, C. W., Allen, C. D., Bell, D. M., Bragg, D. C., et al. (2016). The impacts of increasing drought on forest dynamics, structure, and biodiversity in the United States. *Global Change Biology*, *22*(7), 2329–2352. https://doi.org/10.1111/gcb.13160

Clark, M. P., Fan, Y., Lawrence, D. M., Adam, J. C., Bolster, D., Gochis, D. J., et al. (2015). Improving the representation of hydrologic processes in Earth System Models. *Water Resources Research*, *51*(8), 5929–5956. https://doi.org/10.1002/2015WR017096

Cordes, L., Hughes, F., & Getty, M. (1997). Factors affecting the regeneration and distribution of riparian woodlands along a northern Prairie River: The Red Deer River, Alberta, Canada. *Journal of Biogeography*, *24*(5), 675–695. https://doi.org/10.1111/j.1365-2699.1997.tb00077.x

Dawson, T. E., & Ehleringer, J. R. (1991). Streamside trees that do not use stream water. *Nature*, *350*(6316), 335–337. https://doi.org/10.1038/350335a0

Dijk, A. I., Beck, H. E., Crosbie, R. S., Jeu, R. A., Liu, Y. Y., Podger, G. M., et al. (2013). The Millennium Drought in Southeast Australia (2001–2009): Natural and human causes and implications for water resources, ecosystems, economy, and society. *Water Resources Research*, *49*(2), 1040–1057. https://doi.org/10.1002/wrcr.20123

Dingman, L. S. (1994). *Physical hydrology*. New York: Macmillan Publishing Company.

Fan, Y. (2015). Groundwater in the Earth's critical zone: Relevance to large-scale patterns and processes. *Water Resources Research*, *51*, 3052–3069. https://doi.org/10.1002/2015WR017037

Fan, Y., Miguez-Macho, G., Jobbágy, E. G., Jackson, R. B., & Otero-Casal, C. (2017). Hydrologic regulation of plant rooting depth. *Proceedings of the National Academy of Sciences*, 201712381.

Fang, Y., Leung, L. R., Duan, Z., Wigmosta, M. S., Maxwell, R. M., Chambers, J. Q., & Tomasella, J. (2017). Influence of landscape heterogeneity on water available to tropical forests in an Amazonian catchment and implications for modeling drought response. *Journal of Geophysical Research: Atmospheres*, *122*, 8410–8426. https://doi.org/10.1002/2017JD027066

Farquhar, G., von Caemmerer, S. V., & Berry, J. (1980). A biochemical model of photosynthetic CO_2 assimilation in leaves of C3 species. *Planta*, *149*(1), 78–90. https://doi.org/10.1007/BF00386231

Fisher, R. A., Koven, C. D., Anderegg, W. R., Christoffersen, B. O., Dietze, M. C., Farrior, C., et al. (2017). Vegetation demographics in Earth System Models: A review of progress and priorities. *Global Change Biology*, *24*(1), 35–54.

Flanagan, L. B., Orchard, T. E., Logie, G. S., Coburn, C. A., & Rood, S. B. (2017). Water use in a riparian cottonwood ecosystem: Eddy covariance measurements and scaling along a river corridor. *Agricultural and Forest Meteorology*, *232*, 332–348. https://doi.org/10.1016/j.agrformet.2016.08.024

Fleckenstein, J. H., Niswonger, R. G., & Fogg, G. E. (2006). River-aquifer interactions, geologic heterogeneity, and low-flow management. *Groundwater*, *44*(6), 837–852. https://doi.org/10.1111/j.1745-6584.2006.00190.x

Frei, S., Fleckenstein, J., Kollet, S., & Maxwell, R. (2009). Patterns and dynamics of river–aquifer exchange with variably-saturated flow using a fully-coupled model. *Journal of Hydrology*, *375*(3-4), 383–393. https://doi.org/10.1016/j.jhydrol.2009.06.038

Friedman, J. M., & Lee, V. J. (2002). Extreme floods, channel change, and riparian forests along ephemeral streams. *Ecological Monographs*, *72*(3), 409–425. https://doi.org/10.1890/0012-9615(2002)072[0409:EFCCAR]2.0.CO;2

Hacke, U., Sperry, J., Ewers, B., Ellsworth, D., Schäfer, K., & Oren, R. (2000). Influence of soil porosity on water use in *Pinus taeda*. *Oecologia*, *124*(4), 495–505. https://doi.org/10.1007/PL00008875

Hanson, P. J., Amthor, J. S., Wullschleger, S. D., Wilson, K., Grant, R. F., Hartley, A., et al. (2004). Oak forest carbon and water simulations: Model intercomparisons and evaluations against independent data. *Ecological Monographs*, *74*(3), 443–489. https://doi.org/10.1890/03-4049

Harner, M. J., & Stanford, J. A. (2003). Differences in cottonwood growth between a losing and a gaining reach of an alluvial floodplain. *Ecology*, *84*(6), 1453–1458. https://doi.org/10.1890/0012-9658(2003)084[1453:DICGBA]2.0.CO;2

Hopkinson, C., Chasmer, L. E., Sass, G., Creed, I. F., Sitar, M., Kalbfleisch, W., & Treitz, P. (2005). Vegetation class dependent errors in lidar ground elevation and canopy height estimates in a boreal wetland environment. *Canadian Journal of Remote Sensing*, *31*(2), 191–206. https://doi.org/10.5589/m05-007

Horton, J., Kolb, T., & Hart, S. (2001). Responses of riparian trees to interannual variation in ground water depth in a semi-arid river basin. *Plant, Cell & Environment*, *24*(3), 293–304. https://doi.org/10.1046/j.1365-3040.2001.00681.x

Jackson, R. B., Sperry, J. S., & Dawson, T. E. (2000). Root water uptake and transport: Using physiological processes in global predictions. *Trends in Plant Science*, *5*(11), 482–488. https://doi.org/10.1016/S1360-1385(00)01766-0

Johnson, D. M., Domec, J. C., Berry, Z. C., Schwantes, A. M., Woodruff, D. R., McCulloh, K. A., et al. (2018). Co-occurring woody species have diverse hydraulic strategies and mortality rates during an extreme drought. *Plant, Cell & Environment*, *41*(3), 576–588. https://doi.org/10.1111/pce.13121

Jones, J. E., & Woodward, C. S. (2001). Newton–Krylov-multigrid solvers for large-scale, highly heterogeneous, variably saturated flow problems. *Advances in Water Resources*, *24*(7), 763–774. https://doi.org/10.1016/S0309-1708(00)00075-0

Kattge, J., Diaz, S., Lavorel, S., Prentice, I. C., Leadley, P., Bönisch, G., et al. (2011). TRY—A global database of plant traits. *Global Change Biology*, *17*(9), 2905–2935. https://doi.org/10.1111/j.1365-2486.2011.02451.x

Kollet, S. J., & Maxwell, R. M. (2006). Integrated surface–groundwater flow modeling: A free-surface overland flow boundary condition in a parallel groundwater flow model. *Advances in Water Resources*, *29*(7), 945–958. https://doi.org/10.1016/j.advwatres.2005.08.006

Kollet, S. J., & Maxwell, R. M. (2008). Capturing the influence of groundwater dynamics on land surface processes using an integrated, distributed watershed model. *Water Resources Research*, *44*(2), W02402. https://doi.org/10.1029/2007WR006004

Kollet, S. J., Maxwell, R. M., Woodward, C. S., Smith, S., Vanderborght, J., Vereecken, H., & Simmer, C. (2010). Proof of concept of regional scale hydrologic simulations at hydrologic resolution utilizing massively parallel computer resources. *Water Resources Research*, *46*, W04201. https://doi.org/10.1029/2009WR008730

Kranjcec, J., Mahoney, J. M., & Rood, S. B. (1998). The responses of three riparian cottonwood species to water table decline. *Forest Ecology and Management*, *110*(1-3), 77–87. https://doi.org/10.1016/S0378-1127(98)00276-X

Krause, S., Lewandowski, J., Grimm, N. B., Hannah, D. M., Pinay, G., McDonald, K., et al. (2017). Ecohydrological interfaces as hotspots of ecosystem processes. *Water Resources Research*, *53*(8), 6359–6376. https://doi.org/10.1002/2016WR019516

Leblanc, M., Tweed, S., Van Dijk, A., & Timbal, B. (2012). A review of historic and future hydrological changes in the Murray-Darling Basin. *Global and Planetary Change*, *80*, 226–246.

Leij, F. J., Alves, W. J., and van Genuchten, M. T. (1996). The UNSODA unsaturated soil hydraulic database: User's manual, National Risk Management Research Laboratory, Office of Research and Development, US Environmental Protection Agency.

Lytle, D. A., & Merritt, D. M. (2004). Hydrologic regimes and riparian forests: A structured population model for cottonwood. *Ecology*, *85*(9), 2493–2503. https://doi.org/10.1890/04-0282

Mackay, D. S., Roberts, D. E., Ewers, B. E., Sperry, J. S., McDowell, N. G., & Pockman, W. T. (2015). Interdependence of chronic hydraulic dysfunction and canopy processes can improve integrated models of tree response to drought. *Water Resources Research*, *51*, 6156–6176. https://doi.org/10.1002/2015WR017244

Manzoni, S., Vico, G., Porporato, A., & Katul, G. (2013). Biological constraints on water transport in the soil–plant–atmosphere system. *Advances in Water Resources*, *51*, 292–304. https://doi.org/10.1016/j.advwatres.2012.03.016

Maxwell, R. M. (2013). A terrain-following grid transform and preconditioner for parallel, large-scale, integrated hydrologic modeling. *Advances in Water Resources*, *53*, 109–117. https://doi.org/10.1016/j.advwatres.2012.10.001

Maxwell, R. M., Condon, L., & Kollet, S. (2015). A high-resolution simulation of groundwater and surface water over most of the continental US with the integrated hydrologic model ParFlow v3. *Geoscientific Model Development*, *8*(3), 923–937. https://doi.org/10.5194/gmd-8-923-2015

Maxwell, R. M., & Kollet, S. J. (2008). Interdependence of groundwater dynamics and land-energy feedbacks under climate change. *Nature Geoscience*, *1*(10), 665–669. https://doi.org/10.1038/ngeo315

McDowell, N. G., Fisher, R. A., Xu, C., Domec, J., Hölttä, T., Mackay, D. S., et al. (2013). Evaluating theories of drought-induced vegetation mortality using a multimodel–experiment framework. *New Phytologist*, *200*(2), 304–321. https://doi.org/10.1111/nph.12465

Miguez-Macho, G., & Fan, Y. (2012). The role of groundwater in the Amazon water cycle: 2. Influence on seasonal soil moisture and evapotranspiration. *Journal of Geophysical Research*, *117*(D15), D15114. https://doi.org/10.1029/2012JD017540

Millar, D. J., Ewers, B. E., Mackay, D. S., Peckham, S., Reed, D. E., & Sekoni, A. (2017). Improving ecosystem-scale modeling of evapotranspiration using ecological mechanisms that account for compensatory responses following disturbance. *Water Resources Research*, *53*, 7853–7868. https://doi.org/10.1002/2017WR020823

Mishra, V., Cherkauer, K. A., & Shukla, S. (2010). Assessment of drought due to historic climate variability and projected future climate change in the midwestern United States. *Journal of Hydrometeorology*, *11*(1), 46–68. https://doi.org/10.1175/2009JHM1156.1

Newman, B. D., Wilcox, B. P., Archer, S. R., Breshears, D. D., Dahm, C. N., Duffy, C. J., et al. (2006). Ecohydrology of water-limited environments: A scientific vision. *Water Resources Research*, *42*, W06302. https://doi.org/10.1029/2005WR004141

Phillips, R. P., Ibáñez, I., D'Orangeville, L., Hanson, P. J., Ryan, M. G., & McDowell, N. G. (2016). A belowground perspective on the drought sensitivity of forests: Towards improved understanding and simulation. *Forest Ecology and Management*, *380*, 309–320. https://doi.org/10.1016/j.foreco.2016.08.043

Powell, T. L., Galbraith, D. R., Christoffersen, B. O., Harper, A., Imbuzeiro, H., Rowland, L., et al. (2013). Confronting model predictions of carbon fluxes with measurements of Amazon forests subjected to experimental drought. *New Phytologist*, *200*(2), 350–365. https://doi.org/10.1111/nph.12390

Richards, L. A. (1931). Capillary conduction of liquids through porous mediums. *Physics*, *1*(5), 318–333. https://doi.org/10.1063/1.1745010

Rihani, J. F., Maxwell, R. M., & Chow, F. K. (2010). Coupling groundwater and land surface processes: Idealized simulations to identify effects of terrain and subsurface heterogeneity on land surface energy fluxes. *Water Resources Research*, *46*, W12523. https://doi.org/10.1029/2010WR009111

Rood, S. B., Ball, D. J., Gill, K. M., Kaluthota, S., Letts, M. G., & Pearce, D. W. (2013). Hydrologic linkages between a climate oscillation, river flows, growth, and wood Δ^{13}C of male and female cottonwood trees. *Plant, Cell & Environment*, *36*(5), 984–993. https://doi.org/10.1111/pce.12031

Rood, S. B., Bigelow, S. G., & Hall, A. A. (2011). Root architecture of riparian trees: River cut-banks provide natural hydraulic excavation, revealing that cottonwoods are facultative phreatophytes. *Trees*, *25*(5), 907–917. https://doi.org/10.1007/s00468-011-0565-7

Rood, S. B., Braatne, J. H., & Hughes, F. M. (2003). Ecophysiology of riparian cottonwoods: Stream flow dependency, water relations and restoration. *Tree Physiology*, *23*(16), 1113–1124. https://doi.org/10.1093/treephys/23.16.1113

Rood, S. B., Mahoney, J. M., Reid, D. E., & Zilm, L. (1995). Instream flows and the decline of riparian cottonwoods along the St. Mary River, Alberta. *Canadian Journal of Botany*, *73*(8), 1250–1260. https://doi.org/10.1139/b95-136

Rood, S. B., Pan, J., Gill, K. M., Franks, C. G., Samuelson, G. M., & Shepherd, A. (2008). Declining summer flows of Rocky Mountain Rivers: Changing seasonal hydrology and probable impacts on floodplain forests. *Journal of Hydrology*, *349*(3-4), 397–410. https://doi.org/10.1016/j.jhydrol.2007.11.012

Rood, S. B., Patiño, S., Coombs, K., & Tyree, M. T. (2000). Branch sacrifice: Cavitation-associated drought adaptation of riparian cottonwoods. *Trees*, *14*(5), 0248–0257. https://doi.org/10.1007/s004680050010

Sack, L., Ball, M. C., Brodersen, C., Davis, S. D., Des Marais, D. L., Donovan, L. A., et al. (2016). Plant hydraulics as a central hub integrating plant and ecosystem function: Meeting report for 'Emerging Frontiers in Plant Hydraulics'(Washington, DC, May 2015). *Plant, Cell & Environment*, *39*(9), 2085–2094. https://doi.org/10.1111/pce.12732

Schaller, M. F., & Fan, Y. (2009). River basins as groundwater exporters and importers: Implications for water cycle and climate modeling. *Journal of Geophysical Research*, *114*, D04103. https://doi.org/10.1029/2008JD010636

Schook, D. M., Friedman, J. M., & Rathburn, S. L. (2016). Flow reconstructions in the Upper Missouri River Basin using riparian tree rings. *Water Resources Research*, *52*, 8159–8173. https://doi.org/10.1002/2016WR018845

Scott, M. L., Auble, G. T., & Friedman, J. M. (1997). Flood dependency of cottonwood establishment along the Missouri River, Montana, USA. *Ecological Applications*, *7*(2), 677–690. https://doi.org/10.1890/1051-0761(1997)007[0677:FDOCEA]2.0.CO;2

Scott, M. L., Shafroth, P. B., & Auble, G. T. (1999). Responses of riparian cottonwoods to alluvial water table declines. *Environmental Management*, *23*(3), 347–358. https://doi.org/10.1007/s002679900191

Sheffield, J., & Wood, E. F. (2008). Projected changes in drought occurrence under future global warming from multi-model, multi-scenario, IPCC AR4 simulations. *Climate Dynamics*, *31*(1), 79–105. https://doi.org/10.1007/s00382-007-0340-z

Shen, C., Niu, J., & Phanikumar, M. S. (2013). Evaluating controls on coupled hydrologic and vegetation dynamics in a humid continental climate watershed using a subsurface-land surface processes model. *Water Resources Research*, *49*, 2552–2572. https://doi.org/10.1002/wrcr.20189

Shepherd, A., Gill, K. M., & Rood, S. B. (2010). Climate change and future flows of Rocky Mountain Rivers: Converging forecasts from empirical trend projection and down-scaled global circulation modelling. *Hydrological Processes*, *24*(26), 3864–3877. https://doi.org/10.1002/hyp.7818

Snyder, K. A., & Williams, D. G. (2000). Water sources used by riparian trees varies among stream types on the San Pedro River, Arizona. *Agricultural and Forest Meteorology*, *105*(1-3), 227–240. https://doi.org/10.1016/S0168-1923(00)00193-3

Sperry, J. S., & Love, D. M. (2015). What plant hydraulics can tell us about responses to climate-change droughts. *New Phytologist*, *207*(1), 14–27. https://doi.org/10.1111/nph.13354

Sperry, J. S., Wang, Y., Wolfe, B. T., Mackay, D. S., Anderegg, W. R. L., McDowell, N. G., & Pockman, W. T. (2016). Pragmatic hydraulic theory predicts stomatal responses to climatic water deficits. *The New Phytologist*, *212*(3), 577–589. https://doi.org/10.1111/nph.14059

Swetnam, T. L., Brooks, P. D., Barnard, H. R., Harpold, A. A., & Gallo, E. L. (2017). Topographically driven differences in energy and water constrain climatic control on forest carbon sequestration. *Ecosphere*, *8*(4). https://doi.org/10.1002/ecs2.1797

Tai, X., Mackay, D. S., Anderegg, W. R., Sperry, J. S., & Brooks, P. D. (2017). Plant hydraulics improves and topography mediates prediction of aspen mortality in southwestern USA. *New Phytologist*, *213*(1), 113–127. https://doi.org/10.1111/nph.14098

Taylor, R. G., Scanlon, B., Döll, P., Rodell, M., Van Beek, R., Wada, Y., et al. (2013). Ground water and climate change. *Nature Climate Change*, *3*(4), 322–329. https://doi.org/10.1038/nclimate1744

Thompson, S. E., Harman, C. J., Troch, P. A., Brooks, P. D., & Sivapalan, M. (2011). Spatial scale dependence of ecohydrologically mediated water balance partitioning: A synthesis framework for catchment ecohydrology. *Water Resources Research*, *47*, W00J03. https://doi.org/10.1029/2010WR009998

Toth, J. (1963). A theoretical analysis of groundwater flow in small drainage basins. *Journal of Geophysical Research*, *68*(16), 4795–4812. https://doi.org/10.1029/JZ068i016p04795

Tyree, M. T., Kolb, K. J., Rood, S. B., & Patiño, S. (1994). Vulnerability to drought-induced cavitation of riparian cottonwoods in Alberta: A possible factor in the decline of the ecosystem? *Tree Physiology*, *14*(5), 455–466. https://doi.org/10.1093/treephys/14.5.455

Van Genuchten, M. T. (1980). A closed-form equation for predicting the hydraulic conductivity of unsaturated soils. *Soil Science Society of America Journal*, *44*(5), 892–898. https://doi.org/10.2136/sssaj1980.03615995004400050002x

Venturas, M. D., Sperry, J. S., & Hacke, U. G. (2017). Plant xylem hydraulics: What we understand, current research, and future challenges. *Journal of Integrative Plant Biology*, *59*(6), 356–389. https://doi.org/10.1111/jipb.12534

Western, A. W., Grayson, R. B., Blöschl, G., Willgoose, G. R., & McMahon, T. A. (1999). Observed spatial organization of soil moisture and its relation to terrain indices. *Water Resources Research*, *35*(3), 797–810. https://doi.org/10.1029/1998WR900065

Willms, J., Rood, S. B., Willms, W., & Tyree, M. (1998). Branch growth of riparian cottonwoods: A hydrologically sensitive dendrochronological tool. *Trees*, *12*(4), 215–223. https://doi.org/10.1007/s004680050143

Winter, T. C. (1998). Ground water and surface water: A single resource. *U.S. Geological Survey Circular 1139*. Denver, CO: U.S. government printing office.

Xu, C., McDowell, N. G., Sevanto, S., & Fisher, R. A. (2013). Our limited ability to predict vegetation dynamics under water stress. *New Phytologist*, *200*(2), 298–300. https://doi.org/10.1111/nph.12450

Zimmermann, R. C. (1969). Plant ecology of an arid basin, Tres Alamos-Redington area, southeastern Arizona. Rep. 2330-7102, U.S Government Printing Office.